Photoluminescence Quenching of CdSe Core/Shell Quantum Dots by Hole Transporting Materials

Youlin Zhang,[†,‡,§] Pengtao Jing,[†,‡] Qinghui Zeng,[†,‡] Yajuan Sun,[†] Huaipeng Su,[||] Y. Andrew Wang,[||] Xianggui Kong,[†] Jialong Zhao,[*,†] and Hong Zhang[*,§]

Key Laboratory of Excited State Processes, Changchun Institute of Optics, Fine Mechanics and Physics, Chinese Academy of Sciences, 3888 Eastern South Lake Road, Changchun 130033, China, Graduate School of Chinese Academy of Sciences, Beijing 100039, China, Van't Hoff Institute for Molecular Sciences, University of Amsterdam, Nieuwe Achtergracht 166, 1018 WV Amsterdam, The Netherlands, and Ocean NanoTech, LLC 2143 Worth Lane, Springdale, Arkansas 72764

Received: September 15, 2008; Revised Manuscript Received: December 9, 2008

Photoluminescence quenching of colloidal CdSe core/shell quantum dots (QDs) with CdS, ZnS and CdS/CdZnS/ZnS shells in the presence of hole-transporting materials (HTMs) is studied by means of steady-state and time-resolved photoluminescence spectroscopy. Static quenching is surprisingly found to play an even more important role in the PL quenching process than the dynamic one originating from a hole transfer from QDs to HTMs. The static quenching efficiency of the QDs with single CdS shells of 3 and 6 monolayers is much larger than that of the QDs with a multilayer CdS/CdZnS/ZnS shell. The experimental results are important for understanding the control of the static quenching pathways in QDs by using multishell structures.

Introduction

Semiconductor nanocrystals (NCs), or quantum dots (QDs), are being applied to fabricate hybrid inorganic/organic light-emitting diodes (LEDs) because the QDs exhibit size-tunable photoluminescence (PL), narrow emission line width, high PL quantum yield, superior photostability, and flexible solution-processibility.[1−8] The performance of the QD-based devices is strongly dependent on the structure of the QDs and their surface properties. The effect of organic molecules on the PL properties of CdSe QDs has been widely studied to understand the nature of the QD surface and charge/energy transfer processes between QDs and the organic molecules for further improving the device performance.

The poor photostability of bare-core QDs often causes the wavelength shift of absorption and PL peaks as well as the change of PL line width and intensity, disturbing the unambiguous confirmation of the interaction mechanisms in the core QD−organic molecule systems.[9−12] Recently, the photostability and PL quantum yield of the CdSe core QDs can be improved by growing a CdS or ZnS shell on the CdSe cores to form core/shell NCs.[13−15] More recently, high-quality CdSe-core CdS/CdZnS/ZnS-multishell QDs with a quantum yield of up to 85% have been synthesized by using a successive ion layer adhesion and reaction (SILAR) technique.[16,17] This development raises the question of the shell effect on the charge/energy transfer between QDs and organic molecules.

PL quenching of colloidal CdSe QDs has been widely observed in the presence of organic molecules and polymers.[18−22] In general, the PL quenching includes static and dynamic components. The El-Sayed group attributed the PL to the emission of surface-trapped electrons and holes, assuming that butylamine occupies hole sites to block the surface recombination process, resulting in the reduction of luminescent centers of core QDs.[18,20] The quenching is completely static because the PL lifetime is not changed. Recently, the static quenching in InP core QDs in the presence of a conjugated polymer was attributed to the intermolecular interaction.[21] The static quenching does not have any contribution to the energy/charge transfer process. On the other hand, the Kamat group observed a photoinduced charge transfer between CdSe core NCs and a hole acceptor, *p*-phenylenediamine with a low oxidation potential, which was characterized by a PL quenching and lifetime shortening.[22] While there have been a few reports about ultrafast exciton dissociation in QDs by energy/charge transfer to adsorbed acceptors,[23−25] the contribution of the PL quenching to the charge transfer efficiency between core/shell QDs and the acceptors has not been well understood yet.

In this work, we report steady-state and time-resolved PL spectroscopy of CdSe/CdS, CdSe/ZnS, and CdSe/CdS/CdZnS/ZnS core/shell QDs in chloroform with different concentrations of the hole transporting materials (HTMs), *N*,*N*′-bis(1-naphthyl)-*N*,*N*′-diphenyl-1,1′-biphenyl-4,4′-diamine (NPB), *N*,*N*′-diphenyl-*N*,*N*′-bis(3-methylphenyl)-1,1′-biphenyl-4,4′-diamine (TPD), and 4,4′,4″-tris(*N*-carbazolyl)triphenylamine (TCTA), which are used as hole transporting layers to fabricate efficient QD-LEDs.[2−8] Surprisingly the static and dynamic quenching processes coexist even when the shell thickness reaches 6 monolayers (MLs). Furthermore, we estimate the static and dynamic PL quenching efficiency of the QDs with different shell materials and structures by using a preexponential weighted mean lifetime method.[26,27] Finally we suggest that the use of multishell structures can significantly decrease the static quenching pathways in QDs.

Experimental Section

The CdSe/CdS(3,6 ML), CdSe/ZnS(3 ML,) and CdSe/CdS/CdZnS/ZnS(6 ML) core/shell QDs used in this experiment were

* To whom correspondence should be addressed. Jialong Zhao: phone +86-431-86176029 and e-mail zhaojl@ciomp.ac.cn. Hong Zhang: phone +31-20-5256976 and e-mail h.zhang@uva.nl.
† Changchun Institute of Optics, Fine Mechanics and Physics, Chinese Academy of Sciences.
‡ Graduate School of Chinese Academy of Sciences.
§ Van't Hoff Institute for Molecular Sciences, University of Amsterdam.
|| Ocean NanoTech.

10.1021/jp808190v CCC: $40.75
Published on Web 01/14/2009

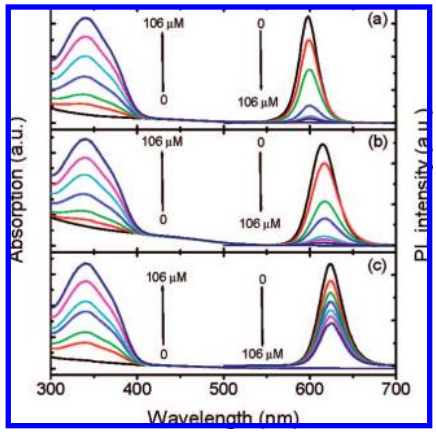

Figure 1. Steady-state absorption and PL spectra of CdSe/CdS(3 ML) (a), CdSe/CdS(6 ML) (b) and CdSe/CdS(3 ML)/CdZnS(1 ML)/ZnS(2 ML) QDs (c) in chloroform solution with different concentrations of NPB, 0, 10.6, 21.2, 42.4, 63.6, 84.8, and 106 μM. Arrows represent the increase of the NPB concentration. Excitation wavelength is 480 nm.

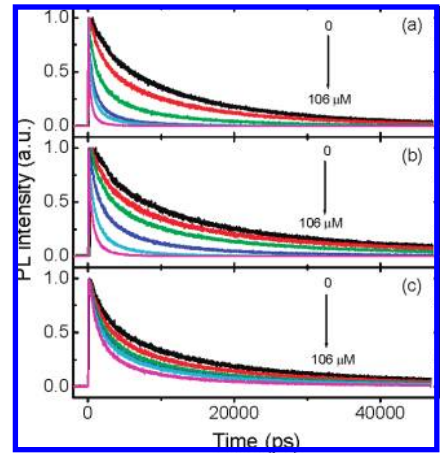

Figure 2. PL decays as a function of time for CdSe/CdS(3 ML) (a), CdSe/CdS(6 ML) (b), and CdSe/CdS(3 ML)/CdZnS(1 ML)/ZnS(2 ML) QDs (c) in chloroform solution with different NPB concentrations, 0, 6.4, 10.6, 21.2, 42.4, and 106 μM from top to bottom as shown in the figure. Excitation wavelength is 450 nm.

synthesized from the same CdSe-core particles with a 3.5 nm diameter by using SILAR method.[16] Their sizes were determined to be about 5.7, 7.4, 5.8, and 8.1 nm, respectively, from transmission electron microscopy (TEM) measurement (Figure S1, Supporting Information). The shell thicknesses were estimated by using one CdS-ML (0.35 nm), one ZnS-ML (0.31nm), and one ZnCdS-ML (0.33 nm) on the basis of the wurzite structure of the respective compounds.[16] Typical PL quantum efficiencies of these samples are 40−70% and the thicknesses of all CdS, CdZnS, and ZnS shells were varied from 1 to 6 MLs. The as-prepared QDs were further purified to remove excess ligands and synthetic byproduct. All QD samples were at least twice washed by dissolution in hexane or chloroform and subsequent precipitation with acetone or methanol followed by drying under N_2. The removal of organic ligands from the core/shell QDs in this experiment caused a drop of the QY by about 20−40% due to reduction of the ligands on the dot surface, compared with unwashed ones, which is consistent with the previous results.[4,16]

Steady-state absorption measurements were carried out with use of a Cary 300 double-beam spectrometer at a spectral resolution of 1 nm. Steady-state PL spectra were measured with the emission spectrometer described previously[28] under excitation at 480 nm. The picosecond fluorescence transient spectroscopy in all samples was measured with a calibrated fluorescence setup outfitted with a time-correlated single-photon-counting (TCSPC) detection system.[28] The excitation wavelength was selected to below the band gap of the HTMs, for example, 450 nm. All experiments were performed at room temperature.

Results and Discussion

Figure 1 shows the steady-state absorption and PL spectra of CdSe/CdS(3 ML), CdSe/CdS(6 ML), and CdSe/CdS(3 ML)/CdZnS(1 ML)/ZnS(2 ML) QDs in chloroform solution with different concentrations of NPB. No significant change in absorption spectra of the CdSe core/shell QDs is observed after NPB is added into the QD solution (Figure S2, Supporting Information). In the meantime, the PL intensity is, however, decreased. As shown in Figure 1, PL quenching with NPB concentration is much faster for CdSe/CdS QDs with a CdS shell of 3 and 6 MLs than for CdSe/CdS(3 ML)/CdZnS(1 ML)/ZnS(2 ML) QDs. Similarly, fast PL quenching of CdSe/ZnS(2 ML) QDs is also observed. A small red shift of about 1−2 nm of PL peak is observed for CdSe/CdS QDs with 3 and 6 MLs CdS shells compared with those of the CdSe QDs in the absence of NPB, but no shift is observed in PL spectra of CdSe core/multishell QDs with the concentration of NPB up to 106 μM (Figure S3, Supporting Information). Moreover, the PL spectral shape is independent of NPB concentration, ruling out the formation of new surface states.[25] This indicates that the PL quenching of the QDs is dependent not only on the thickness of the shell, but also on the structure of the shell.

The PL decay dynamics of the CdSe core/shell QDs in the absence and presence of different concentrations of NPB are shown in Figure 2. The QDs exhibit significant PL lifetime shortening with increasing NPB concentration. The PL lifetime decay curves of CdSe core/shell QDs at different concentrations of NPB can be well fitted by a triexponential function defined as $I(t) = A_1 \exp(-t/\tau_1) + A_2 \exp(-t/\tau_2) + A_3 \exp(-t/\tau_3)$, where τ_1, τ_2, and τ_3 are the time constants, and A_1, A_2, and A_3 are the normalized amplitudes of the components, respectively.[29] The average lifetimes τ_{AV}, determined by the expression $\tau_{AV} = (A_1\tau_1^2 + A_2\tau_2^2 + A_3\tau_3^2)/(A_1\tau_1 + A_2\tau_2 + A_3\tau_3)$, are also summarized in Tables S1−S3 (Supporting Information), where it is clearly shown that adding the HTMs into CdSe core/shell QD solution quenches the PL and also results in a significant decrease of the average PL lifetime. For example, the average PL lifetime of the CdSe/CdS(6 ML) QDs significantly changes from 30.57 to 1.46 ns when the NPB concentration is increased from 0 to 106 μM whereas such a concentration change leads to only a small variation in the average lifetime, e.g., from 19.43 to 10.46 ns, for CdSe/CdS(3 ML)/CdZnS(1 ML)/ZnS(2 ML) QDs. This result demonstrates that the PL lifetime quenching also depends on the thickness and structure of the shell.

Figure 3 shows the intensity ratio (I_0/I) and average lifetime (τ_{AV0}/τ_{AV}) of the CdSe/CdS(6 ML) and CdSe/CdS(3 ML)/CdZnS(1 ML)/ZnS(2 ML) QD PL as a function of NPB concentration. The subscript 0 denotes the parameters (intensity or lifetime of QD PL or amplitude of PL lifetime) in the absence of quencher. As is well-known, the majority of PL quenching results are explained by the Stern−Volmer equation $I_0/I = 1 + K_{SV}[Q]$, where K_{SV} is the Stern−Volmer constant and [Q] is concentration of the quencher.[20,22] However, the plots of I_0/I versus quencher concentration in this experiment do not fit this conventional linear Stern−Volmer equation. The plots in Figure

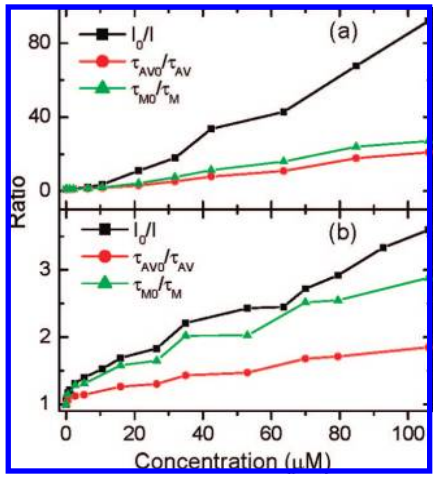

Figure 3. I_0/I and τ_{AV0}/τ_{AV} of CdSe/CdS(6 ML) (a) and CdSe/CdS(3 ML)/CdZnS(1 ML)/ZnS(2 ML) QDs (b) as a function of NPB concentration. τ_{M0}/τ_M is also plotted in the figure for comparison.

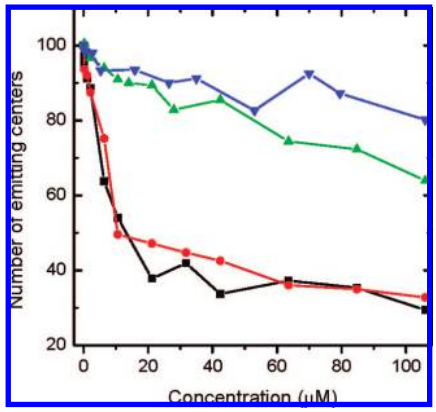

Figure 4. The number of emitting centers of CdSe QDs shelled with CdS(3 ML) (black squares), CdS(6 ML) (red circles), CdS(2 ML)/CdZnS(2 ML)/ZnS(2 ML) (green vertical triangles), and CdS(3 ML)/CdZnS(1 ML)/ZnS(2 ML) (blue converse triangles) as a function of NPB concentration.

3 indicate that both dynamic and static quenching processes occur in the QD-NPB system or there are multiple PL pathways with different quenching efficiency.[30−33] Moreover, the relationship between lifetime quenching ratio and NPB concentration is also nonlinear. In particular, the quenching ratio τ_{AV0}/τ_{AV} is smaller than that of PL intensity, depending on the shell structure of the QDs.

We ascertain the relative contributions of static and dynamic quenching by a relation $I_0/I = N_0/N \times \tau_{M0}/\tau_M$, where τ_M is the pre-exponential weighted mean lifetime[26,27] determined by an expression $\tau_M = (A_1\tau_1 + A_2\tau_2 + A_3\tau_3)/(A_1 + A_2 + A_3)$ as listed in Tables S1−S3 (Supporting Information), and N_0 and N are the assumed emitting centers in the absence and presence of HTMs. Therefore, it is true for the following expression $I_0/I = \tau_{M0}/\tau_M$ if there is no static quenching, namely $N = N_0$, which has been demonstrated experimentally.[26,27] τ_{M0}/τ_M as a function of NPB concentration is also shown in Figure 3. It is clear that there appear static and dynamic components in the above quenching process. Furthermore, according to the formula $I_0/I = N_0/N \times \tau_{M0}/\tau_M$,[26,27] we can estimate the number of emitting centers (N) in the core/shell QDs as a function of NPB concentration as shown in Figure 4 by assuming that the number of emitting centers $N_0 = 100$ in the absence of the quencher. As seen in Figure 4, the number of emission centers in CdSe/CdS core/shell QDs rapidly decreases with increasing the NPB

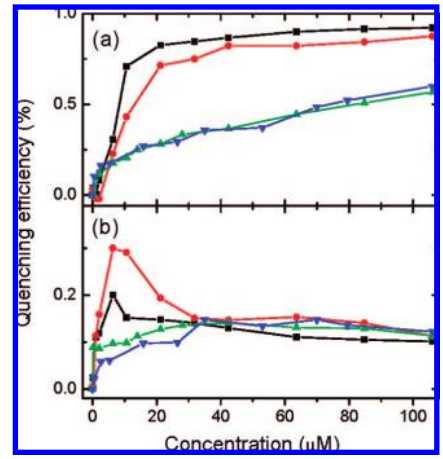

Figure 5. Static (a) and dynamic quenching efficiencies (b) of CdSe QDs shelled with CdS(3 ML) (black squares), CdS(6 ML) (red circles), CdS(2 ML)/CdZnS(2 ML)/ZnS(2 ML) (green vertical triangles), and CdS(3 ML)/CdZnS(1 ML)/ZnS(2 ML) (blue converse triangles) as a function of NPB concentration.

concentration from 0 to 10 μM, compared with those of the QDs with multishells. Hence, the static quenching resulting from the decrease of the number in the emitting centers plays an important role in the PL quenching of the core/shell QDs in the presence of the NPB molecules, which is strongly dependent on the shell thickness and structure. The static and dynamic quenching efficiencies Q_S and Q_D can be estimated by the following expressions:

$$Q_S = \Delta I_S/I_0 = [(A_{10} - A_1 \times N/N_0)\tau_{10} + (A_{20} - A_2 \times N/N_0)\tau_{20} + (A_{30} - A_3 \times N/N_0)\tau_{30}]/(A_{10}\tau_{10} + A_{20}\tau_{20} + A_{30}\tau_{30}) \quad (1)$$

$$Q_D = \Delta I_D/I_0 = (I_0 - I - \Delta I_S)/I_0 = [A_1(\tau_{10} - \tau_1) + A_2(\tau_{20} - \tau_2) + A_3(\tau_{30} - \tau_3)] \times N/N_0/(A_{10}\tau_{10} + A_{20}\tau_{20} + A_{30}\tau_{30}) \quad (2)$$

where ΔI_S and ΔI_D are the intensity changes due to the static and dynamic quenching at different concentrations, respectively. The calculated quenching efficiencies of CdSe QDs shelled with CdS(3 ML), CdS(6 ML), CdS(2 ML)/CdZnS(2 ML)/ZnS(2 ML), and CdS(3 ML)/CdZnS(1 ML)/ZnS(2 ML) as a function of NPB concentration are shown in Figure 5. The static quenching efficiency of the QDs rapidly increases with the NPB concentration in the range of 0−10 μM, and reaches the maximum of about 80% at the concentration of about 30 μM while the efficiency of CdSe multishell QDs is much lower than that of CdSe/CdS(3, 6 ML) core/shell QDs. On the other hand, the dynamic quenching efficiency of CdSe/CdS core/shell QDs increases rapidly and reaches the maximum at a relatively low concentration of NPB. This is because NPB molecules modify the surface of the QDs to increase the number of long lifetime (τ_1) luminescent centers (Tables S1 and S2, Supporting Information), which is supported by the negative static quenching efficiency. Further increasing the NPB concentration leads to a rapid drop of the dynamic quenching efficiencies of all QDs and they reach the saturated value of about 15%. The rapid increase of the static quenching efficiency with the concentration of NPB as seen in Figure 5 corresponds to a decrease in the number of the luminescent centers, resulting in a weak dependence of the dynamic quenching efficiency on the QD shell structure. Similarly, the PL quenching and lifetime

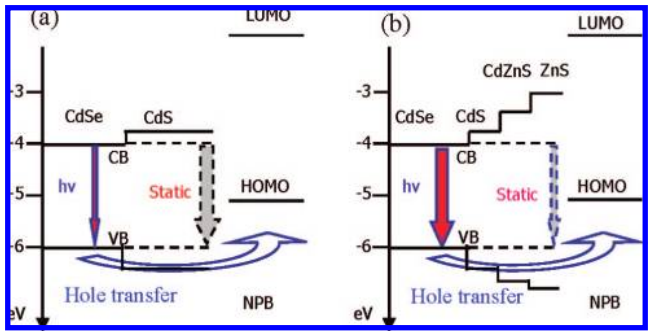

Figure 6. Schematic diagrams of PL quenching mechanisms for CdSe/CdS (a) and CdSe/CdS/CdZnS/ZnS core/shell QDs (b) in the presence of HTMs. The electronic level structure of the CdSe core/shell QDs and HOMO and LUMO levels of the HTMs are taken from previous data.[1,3,4,7,8]

shortening of the core/shell QDs is confirmed in the presence of TPD and TCTA. The efficiencies of PL intensity and lifetime quenching decrease with decreasing the energy difference between the valence band of the QDs and HOMO levels of NPB (−5.1 eV), TPD (−5.3 eV), and TCTA (−5.7 eV). The static and dynamic quenching efficiencies of the CdSe core/shell QDs were also estimated based on eqs 1 and 2 as shown in Figure S4 (Supporting Information).

Figure 6 shows the schematic diagram of electronic levels and structure of the CdSe core/shell QDs and HOMO and LUMO levels of the HTMs, where NPB is taken as an example. There are five possible pathways for the NPB molecules to quench the QD PL:[22−25] (1) energy transfer from QDs to HTM molecules; (2) electron transfer from HTM molecules to QDs; (3) the formation of new radiative and nonradiative centers; (4) static quenching (the decrease in the number of the emitting centers); and (5) dynamic quenching (hole transfer from QDs to HTM molecules). The energy transfer from QDs to HTM is not possible based on their absorption and PL spectra. Another pathway that is also not possible is the electron transfer from the HTMs to QDs because the excitation wavelength was selected such that HTM molecules were not excited. No significant change in peak position and line width of the PL spectra (Figures S2 and S3, Supporting Information) indicates that no new emitting state forms in the QD-HTM system. In addition, no new fast recombination process such as electron trapping at the interface between QDs and HTMs is confirmed by the transient absorption spectroscopy of the QDs. Therefore, the PL quenching might only come from the remaining two possible pathways: static and dynamic quenching.

The surface-related emissions are often considered to be a dominant radiative recombination process in the naked QDs.[31−33] This process in the core/shell QDs should be decreased significantly after a semiconductor shell is grown on a CdSe core to passivate the surface of core and confine most of the electrons and holes in the cores. However, a large amount of static quenching was surprisingly confirmed in the core/shell QDs in our experiment. The pathway of the static quenching can be rationalized as follows: First, there still appear some Zn^{2+} or Cd^{2+} hole sites on the ZnS or CdS shell surface in the core/shell QDs.[15,32,33] The HTM molecules might occupy the Zn^{2+} or Cd^{2+} hole site to block the recombination process, resulting in the static quenching. Second, PL properties of the QDs are sensitive to the environment of the shells on the QD surface.[16] As a result, the emitting states near the QD surface are easily removed by the HTMs that adsorbed on the surface of the QDs, resulting in a significant static PL quenching. The origin of producing the above pathways comes from expanding the electron wave function,[14,34] so the static quenching should be related to the confinement barrier height, shell thickness, and lattice match between CdSe cores and CdS, CdZnS, or ZnS shells. The density of the emitting states in a ZnS shell is expected to be lower than that in a CdS shell because of a larger barrier between the conduction bands of the CdSe core and ZnS shell. This also explains that the static quenching efficiency of core/multishell QDs is much lower than that of CdSe/CdS core/shell QDs. But we observed also large static quenching in the CdSe/ZnS core/shell QDs. This might reflect the fact that a high quality of ZnS shell structure is hard to reach, considering the large lattice mismatch between the CdSe core and the ZnS shell.[35] The smallest amount of static quenching has thus been observed in CdSe/CdS/CdZnS/ZnS core/multishell QDs due to the high quality of the multishells.[16] As seen in Figure 6, for the CdSe/CdS(6 ML) QDs a large part of the luminescent centers are eliminated by static quenching, and only a small part of them take part in hole transfer; for the CdSe/CdS(3 ML)/CdZnS(1 ML)/ZnS(2 ML) core/multishell QDs a small part of the luminescent centers are eliminated by static quenching, and most part of them take part in hole transfer. But the lifetime quenching of CdSe/CdS(6 ML) QDs is higher than that of the multishell ones. As seen in Figures 5 and S4 (Supporting Information), the dynamic quenching efficiencies depend not only on the shell structure of QDs but also the HTM molecules.

Conclusions

In summary, the efficiency of the PL quenching in QDs is strongly dependent on the structure of the shells and the HOMO levels of the HTMs. Surprisingly, a majority of the QDs in the QD-HTM solution are quenched completely via static quenching pathways while only a small part of them experience the dynamic charge transfer/charge separation. It is hypothesized that improvement in quantum efficiency of QD-LEDs could be achieved by careful modification of the nanocrystal surface with functional organic molecules, such as HTMs. However, the static quenching would decrease the PL quantum efficiency of the QDs, resulting in a low quantum efficiency of QD-LEDs fabricated by doping QDs into organic molecules/polymers. On the other hand, the large static quenching also causes a decrease in charge transfer efficiency for efficient QD solar cells. Therefore, it is necessary to effectively decrease the static quenching pathways by using a multishell to passivate the QD surface or selecting organic molecules on the QD surface to prevent the removal of the emitting centers for improving the performance of QD-based devices.

Acknowledgment. This work was supported by the program of CAS Hundred Talents, the National Natural Science Foundation of China (60771051, 60601015, 60601014, 10674132, 20603035, and 10874179), the National High Technology Development Program (2006AA03Z335), NSF SBIR 0638209 (USA), and the exchange program between CAS of China and KNAW of The Netherlands. J.Z. gratefully acknowledges Prof. Alex K.-Y. Jen for his helpful discussion.

Supporting Information Available: TEM images, enlarged absorption spectra near the first exciton absorption peaks, enlarged PL spectra, static and dynamic quenching efficiencies, the fitted time constants, amplitudes, and calculated lifetimes.

This material is available free of charge via the Internet at http://pubs.acs.org.

References and Notes

(1) Colvin, V. L.; Schlamp, M. C.; Alivisatos, A. P. *Nature* **1994**, *370*, 354.
(2) Dabbousi, B. O.; Bawendi, M. G.; Onitsuka, O.; Rubner, M. F. *Appl. Phys. Lett.* **1995**, *66*, 1316.
(3) Coe, S.; Woo, W. K.; Bawendi, M.; Bulovic, V. *Nature* **2002**, *420*, 800.
(4) Zhao, J. L.; Bardecker, J. A.; Munro, A. M.; Liu, M. S.; Niu, Y. H.; Ding, I. K.; Luo, J. D.; Chen, B. Q.; Jen, A. K.-Y.; Ginger, D. S. *Nano Lett.* **2006**, *6*, 463.
(5) Sun, Q. J.; Wang, Y. A.; Li, L. S.; Wang, D. Y.; Zhu, T.; Xu, J.; Yang, C. H.; Li, Y. F. *Nat. Photon.* **2007**, *1*, 717.
(6) Coe-Sullivan, S.; Steckel, J. S.; Woo, W. K.; Bawendi, M. G.; Bulovic, V. *Adv. Funct. Mater.* **2005**, *15*, 1117.
(7) Niu, Y. H.; Munro, A. M.; Cheng, Y. J.; Tian, Y. Q.; Liu, M. S.; Zhao, J. L.; Bardecker, J. A.; Plante, I. J. L.; Ginger, D. S.; Jen, A. K.-Y. *Adv. Mater.* **2007**, *19*, 3371.
(8) Zhao, J. L.; Zhang, J. Y.; Jiang, C. Y.; Bohnenberger, J.; Basche, T.; Mews, A. *J. Appl. Phys.* **2004**, *96*, 3206.
(9) Nazzal, A. Y.; Wang, X. Y.; Qu, L. H.; Yu, W.; Wang, Y. J.; Peng, X. G.; Xiao, M. *J. Phys. Chem. B* **2004**, *108*, 5507.
(10) Kalyuzhny, G.; Murray, R. W. *J. Phys. Chem. B* **2005**, *109*, 7012.
(11) Bullen, C.; Mulvaney, P. *Langmuir* **2006**, *22*, 3007.
(12) Munro, A. M.; Plante, I. J. L.; Ng, M. S.; Ginger, D. S. *J. Phys. Chem. C* **2007**, *111*, 6220.
(13) Hines, M. A.; Guyot-Sionnest, P. *J. Phys. Chem.* **1996**, *100*, 468.
(14) Peng, X. G.; Schlamp, M. C.; Kadavanich, A. V.; Alivisatos, A. P. *J. Am. Chem. Soc.* **1997**, *119*, 7019.
(15) Dabbousi, B. O.; Rodriguez-Viejo, J.; Mikulec, F. V.; Heine, J. R.; Mattoussi, H.; Ober, R.; Jensen, K. F.; Bawendi, M. G. *J. Phys. Chem. B* **1997**, *101*, 9463.
(16) Xie, R. G.; Kolb, U.; Li, J. X.; Basché, T.; Mews, A. *J. Am. Chem. Soc.* **2005**, *127*, 7480.
(17) Talapin, D. V.; Mekis, I.; Götzinger, S.; Kornowski, A.; Benson, O.; Weller, H. *J. Phys. Chem. B* **2004**, *108*, 18826.
(18) Landes, C.; Burda, C.; Braun, M.; El-Sayed, M. A. *J. Phys. Chem. B* **2001**, *105*, 2981.
(19) Schmelz, O.; Mews, A.; Basche, T.; Herrmann, A.; Muellen, K. *Langmuir* **2001**, *17*, 2861.
(20) Landes, C. F.; Braun, M.; El-Sayed, M. A. *J. Phys. Chem. B* **2001**, *105*, 10554.
(21) Selmarten, D.; Jones, M.; Rumbles, G.; Yu, P.; Nedeljkovic, J.; Shaheen, S. *J. Phys. Chem. B* **2005**, *109*, 15927.
(22) Sharma, S. N.; Pillai, Z. S.; Kamat, P. V. *J. Phys. Chem. B* **2003**, *107*, 10088.
(23) Greenham, N. C.; Peng, X. G.; Alivisatos, A. P. *Phys. Rev. B* **1996**, *54*, 17628.
(24) Ginger, D. S.; Greenham, N. C. *Phys. Rev. B* **1999**, *59*, 10622.
(25) Neuman, D.; Ostrowski, A. D.; Mikhailovsky, A. A.; Absalonson, R. O.; Strouse, G. F.; Ford, P. C. *J. Am. Chem. Soc.* **2008**, *130*, 168.
(26) Carraway, E. R.; Demas, J. N.; DeGraff, B. A. *Anal. Chem.* **1991**, *63*, 332.
(27) Carraway, E. R.; Demas, J. N.; DeGraff, B. A.; Bacon, J. R. *Anal. Chem.* **1991**, *63*, 337.
(28) Tian, L. J.; Sun, Y. J.; Yu, Y.; Kong, X. G.; Zhang, H. *Chem. Phys. Lett.* **2008**, *452*, 188.
(29) Morello, G.; Anni, M.; Cozzoli, P. D.; Manna, L.; Cingolani, R.; De Giorgi, M. *J. Phys. Chem. C* **2007**, *111*, 10541.
(30) Efros, Al. L.; Rosen, M.; Kuno, M.; Nirmal, M.; Norris, D. J.; Bawendi, M. G. *Phys. Rev. B* **1996**, *54*, 4843.
(31) Bawendi, M. G.; Carroll, P. J.; Wilson, W. L.; Brus, L. E. *J. Chem. Phys.* **1992**, *96*, 946.
(32) Wang, X. Y.; Qu, L. H.; Zhang, J. Y.; Peng, X. G.; Xiao, M. *Nano Lett.* **2003**, *3*, 1103.
(33) Califano, M.; Franceschetti, A.; Zunger, A. *Nano Lett.* **2005**, *5*, 2360.
(34) Schooss, D.; Mews, A.; Eychmuller, A.; Weller, H. *Phys. Rev. B* **1994**, *49*, 17072.
(35) Yu, Z. H.; Guo, L.; Du, H.; Krauss, T.; Silcox, J. *Nano Lett.* **2005**, *5*, 565.

JP808190V